CARBON-13 FOURIER TRANSFORM NMR STUDIES IN 20 mm SAMPLE TUBES: OBSERVATION OF INDIVIDUAL CARBON SITES IN PROTEINS

A. Allerhand,[*] R. F. Childers, and E. Oldfield [†]

Department of Chemistry
Indiana University [‡]
Bloomington, Indiana 47401

INTRODUCTION

With the increase in spectrometer sensitivity made available by the development of Fourier transform nmr spectrometers, the ^{13}C nucleus at natural abundance has become less forbidding as a nonperturbing structural probe for biopolymers in solution. In 1970, Allerhand and coworkers [1] reported the first ^{13}C Fourier transform nmr spectrum of a protein, bovine pancreatic ribonuclease A. Since then, a number of other natural-abundance ^{13}C Fourier transform nmr studies of proteins have been published.[2-7] Unfortunately, all these studies have one thing in common: there is no observation of *single-carbon* resonances. Obviously, the ability to monitor single-carbon sites of a protein in solution would significantly improve the applicability of nmr for conformational studies. It should be noted that proton nmr spectra of proteins yield extremely few single-hydrogen resonances.[8] The greater range of ^{13}C chemical shifts [9] is an incentive for trying to use ^{13}C nmr for studying biopolymers in solution.

There are two basic requirements for monitoring single-carbon sites. First, the spectral signal-to-noise ratio after a reasonably short period of digital accumulation of data (say one day) must be sufficient for detecting single-carbon resonances at the low molar concentrations (15 mM and less) that are dictated by the high molecular weights of even the smallest proteins. The signal-to-noise ratio will, of course, be determined both by instrumental characteristics such as magnetic field and sample-tube size, and by sample characteristics such as spin-spin relaxation times (T_2), spin-lattice relaxation times (T_1), and the extent of the nuclear Overhauser enhancement (NOE) which arises upon proton decoupling.[10, 11] The second factor that will determine whether or not one can observe single-carbon resonances of proteins is spectral resolution, which will be a function of magnetic field strength, line widths, and chemical shift nonequivalence. The great range of ^{13}C chemical shifts of amino acids [12] does not ensure sufficient resolution for

observing single-carbon resonances in proteins. In the first place, chemical shift nonequivalence arising from folding of the protein into its native conformation is required, unless there is only one residue of a particular amino acid. Secondly, one must take into account that protein resonances may be much broader than the corresponding resonances of amino acids (see below). In the next section, we shall discuss the various factors that will determine whether or not single-carbon resonances of proteins can be observed. Then, we shall describe our observation of single-carbon resonances of hen egg-white lysozyme and horse-heart cytochrome *c*.

NUCLEAR OVERHAUSER ENHANCEMENT

The signal-to-noise ratio in nmr spectroscopy is influenced by many factors. We will only discuss those of greatest interest in ^{13}C nmr. The combination of low natural-abundance and small gyromagnetic ratio (about one-fourth that of ^1H) yields a basic sensitivity in natural-abundance ^{13}C nmr about 6,000 times lower than in proton nmr spectroscopy.[9] Proton decoupling not only simplifies ^{13}C spectra, but may produce up to a factor of three improvement in signal-to-noise ratio because of the nuclear Overhauser enhancement (NOE).[10] In this way, ^{13}C nmr would only have 2,000 times lower sensitivity than proton nmr. Unfortunately, the maximum NOE of 2.988[10] is not always reached, not because of instrumental limitations, but because of basic molecular properties.[10, 11]

It is not surprising that more effort has gone into increasing instrumental sensitivity in ^{13}C nmr than in proton nmr. Digital signal averaging is often used in proton nmr, but it is essential for most ^{13}C nmr studies. Furthermore, while sample tubes of 5 mm outside diameter are standard on most high-resolution proton nmr spectrometers, diameters of 10 mm, 12 mm, and 13 mm are used on ^{13}C nmr spectrometers. Finally, the Fourier transform technique[12] has greatly shortened the time required to achieve a given signal-to-noise ratio. It is generally accepted that 10 mM is the lowest practical concentration for observing single-carbon resonances at natural abundance on commercial Fourier transform nmr spectrometers,[11] when the maximum NOE of 3 is achieved. In the absence of any NOE, the lower limit is 30 mM, which would prevent the observation of single-carbon resonances in ^{13}C spectra of protein solutions.

Two conditions must be satisfied in order to observe the full NOE of 2.988 upon proton decoupling. First, ^{13}C relaxation must occur entirely by ^{13}C-^1H dipole-dipole interactions. If other relaxation mechanisms are important, the NOE is reduced.[10] It has been shown[13] that when dealing with large molecules, the ^{13}C-^1H dipolar relaxation mechanism is overwhelmingly dominant for carbons with one or more directly attached hydrogens. Non-protonated carbons of proteins may have contributions to their relaxation from chemical shift anisotropy,[14] especially at high magnetic field strengths. The second condition that must be satisfied in order to get the maximum NOE is that the effective correlation time for rotational reorientation (τ_{eff}) of the vectors connecting the ^{13}C nucleus to the ^1H nuclei causing dipolar relaxation must be small relative to the proton resonance frequency (ω_H) in rad/sec:

$$\tau_{eff}\omega_H \ll 1 \tag{1}$$

This "extreme narrowing condition" is normally satisfied for small molecules, because the correlation time for overall rotational reorientation (τ_R) in solution is usually in the range 10^{-12}–10^{-10} sec. In the case of biopolymers in their native conformation, however, τ_R is 10^{-8} sec or greater and Equation 1 will not be satisfied, unless τ_{eff} is dominated by fast internal reorientations. Thus, it is conceivable that we may find smaller NOE values for α carbons of a native protein than for mobile side-chain carbons such as the ε carbons of lysine residues. Furthermore, we might find an increase in the NOE values of α-carbon resonances upon denaturation of a protein.[2]

For the simple case of a ^{13}C-^{1}H group, which is part of a rigid molecule undergoing isotropic rotational reorientation, it is easy to calculate [10, 11, 17] the NOE as a function of τ_R. Results are shown in FIGURE 1 for the case of purely dipolar relaxation, at three commonly used magnetic field strengths (in kG). FIGURE 1 should apply to the α-carbons of a native globular protein, which are thus expected to have the minimum NOE of 1.153.[10, 11] These results will also apply to side-chain carbons whose internal rotations are not fast enough to contribute to τ_{eff}, e.g., the methylene carbons of proline residues, and aromatic side-chain carbons.[18] If internal rotations are fast, a NOE of 2 or more is possible. The actual functional relationship is complex.[11] FIGURE 2 shows the computed NOE (at 14.1 kG) for a tetrahedral carbon with one attached hydrogen, when the C-H vector is undergoing internal rotation with a correlation time τ_G, while attached to a molecule undergoing isotropic rotational reorientation with a correlation time τ_R. Details have been given elsewhere.[11] For side-chain carbons with more than one degree of internal freedom, the situation becomes more complex. Experimental NOE studies of homopolymeric polypeptides in helical conformations indicate that the NOE may reach the maximum value of 2.988 for aliphatic side-chain carbons far
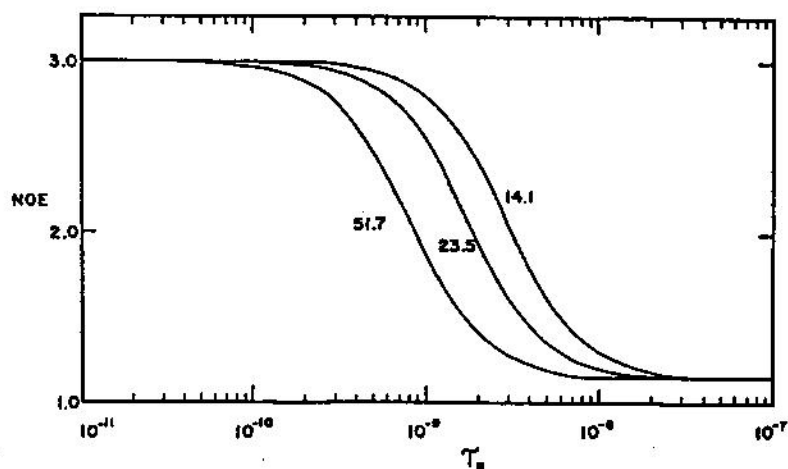

FIGURE 1. Semilog plot of the NOE vs. τ_R (in sec) for a ^{13}C nucleus relaxing by a dipolar interaction with a single proton 1.09 Å away (typical directly bonded C-H distance); in the case of isotropic rotational reorientation, and under conditions of complete proton decoupling.[11] Results are shown for three magnetic fields (in kG).
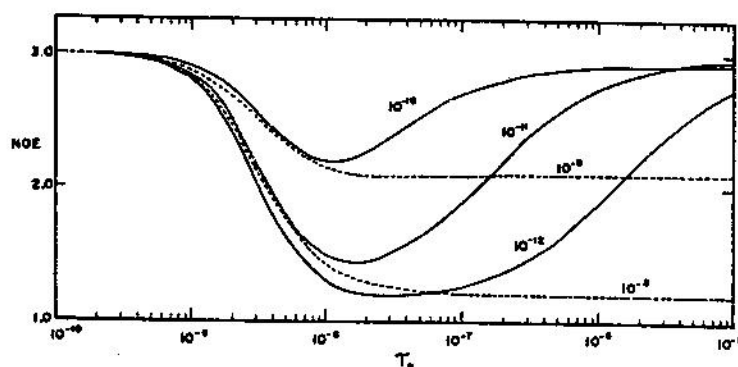
FIGURE 2. Semilog plot of the NOE vs. τ_R (in sec) for the ^{13}C nucleus of a C-H group ($r_{CH} = 1.09$ Å) undergoing internal rotation, attached to a molecule with isotropic rotational reorientation, and under conditions of complete proton decoupling, at 14.1 kG. Number next to each curve is τ_G (in sec.)[11] A tetrahedral angle between the C-H vector and the axis of internal rotation has been assumed.

removed from the backbone.[18] Upon protein denaturation, segmental motions of the backbone become sufficiently fast to dominate τ_{eff} and to satisfy approximately the extreme narrowing condition (Equation 1).[2] Thus, protonated carbons of a denatured protein, including the α carbons, may have a large NOE, as is found for the α carbons of random-coil homopolymeric polypeptides.[19] The NOE of a nonprotonated carbon of a denatured protein will depend on the extent that chemical shift anisotropy contributes to the ^{13}C relaxation.

LINE WIDTHS

FIGURE 3 shows the effect of τ_R and magnetic field on the line width, $W = 1/\pi T_2$, in Hz, for a methine carbon undergoing purely ^{13}C-^1H dipolar relaxation. As in FIGURE 1, we assume here that the methine group is part of a rigid molecule undergoing isotropic rotational reorientation. Details have been given elsewhere.[11] Even for the smallest proteins (ca. 10,000 MW) in their native conformation, our calculations predict a line width of more than 20 Hz at 14.1 kG (and more than 10 Hz at 51.7 kG) for α carbons and side-chain methine carbons not undergoing fast internal rotation. To calculate the line widths of methylene and methyl side-chain carbons not undergoing internal rotation, multiply the line widths of FIGURE 3 by two and three, respectively.[10, 11]

What carbons, if any, of a native protein in solution are expected to have narrow ^{13}C resonances, relative to the α-carbon line widths? Nonprotonated carbons will have much narrower lines than α carbons, even if they have the same τ_{eff} as the α carbons, because the dipolar contribution to $1/T_2$ is inversely proportional to the sixth power of the carbon-hydrogen distance,[10] which is 1.09 Å for directly bonded C-H groups, but about 2 Å or more for nonbonded carbon-hydrogen interactions. Also, protonated side-chain carbons will have appreciably narrower lines than predicted on the basis of FIGURE 3
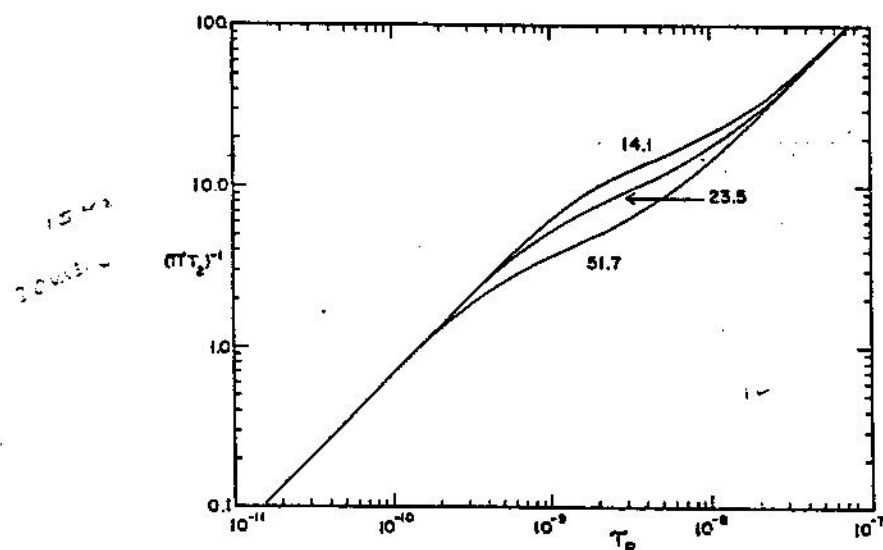
FIGURE 3. Log-log plot of the natural line width $W = 1/\pi T_2$ (in Hz) vs. τ_R (in sec). (See legend of FIGURE 1 and Reference 11 for details.)

if internal motions are faster than overall reorientation of the native protein molecule. The line width will depend on the number of directly attached hydrogens, the rates of overall rotation, the number of degres of internal freedom, the rates of internal rotation, and the bond angles. FIGURE 4 shows calculated line widths (in Hz, at 14.1 kG) for a tetrahedral carbon with one attached hydrogen and one degree of internal motion, when the overall molecular reorientation is isotropic. These theoretical results should be applicable to β carbons, if one multiplies the line widths of FIGURE 3 by the number of directly attached hydrogens. Actual predictions of β-carbon line widths would require a knowledge of the correlation time for internal rotation about the C^α-C^β bond, and about any deviation from tetrahedral bond angles. FIGURE 4 cannot be used for side-chain carbons with more than one degree of internal freedom. One does expect, however, a progressive line narrowing when going from C^β to C^γ and beyond, along an aliphatic side chain.[15, 19-21] For example, the ϵ carbons of lysine residues have very narrow ^{13}C resonances.[2, 6] No significant internal motions are expected for the methylene carbons of proline residues, which should have about twice the line width of the α carbons. Also, internal rotation about C^α-C^β and about C^β-C^γ bonds of aromatic residues is probably too slow in most cases to produce significant line-narrowing.[18] In proton nmr studies of proteins, the ϵ_1 protons of histidine residues (hydrogen at C-2 of the imidazole ring) are often resolved as narrow single-hydrogen resonances.* In contrast, the ϵ_1 carbons are expected to yield broad resonances. This difference is a result of the very short C-H bond distance, relative to the distances involved in the ^1H-^1H dipolar relaxation of the ϵ_1 proton. The dipolar contribution to the line width is proportional to the square of the gyromagnetic ratios and inversely proportional to the sixth power of the distance. The much shorter C-H distance yields a broader ϵ_1-carbon resonance than the ϵ_1-proton

resonance, even though the gyromagnetic ratio of the ^{13}C nucleus is only about a quarter that of the proton.

Upon denaturation, as a result of segmental motion of the protein backbone, there is a dramatic narrowing of ^{13}C resonances of those protonated carbons which yielded broad ^{13}C peaks for the native protein.[2] In contrast, the ϵ carbons of lysine residues appear to have about the same line widths in native and denatured proteins[2] because τ_{eff} for these carbons is dominated by several degrees of internal rotation, which seem to occur at comparable rates in the native and denatured protein.

SPIN-LATTICE RELAXATION TIMES

Spin-lattice relaxation times are pertinent to our discussion because optimum signal-to-noise ratios are achieved when $T_1 W^*$ is at a minimum.[13] Here W^* is the total experimental line width, given by

$$W^* = W + W' \tag{2}$$

where W is the natural line width $(1/\pi T_2)$ and W' is the line-broadening arising from magnetic field inhomogeneity and other instrumental imperfections.

FIGURE 5 shows computed dipolar T_1 values for a methine carbon of a rigid molecule undergoing isotropic rotational reorientation. In the extreme narrowing limit (Equation 1), T_1 is independent of magnetic field, and equal to T_2. For the α carbons and other nonmobile carbons of a native protein $(\tau_R \gtrsim 10^{-8}$ sec), the T_1/T_2 ratio is greater than unity, and increases as τ_R increases. This is an unfavorable situation for good signal-to-noise ratios.[13] It is also apparent when comparing FIGURE 3 with FIGURE 5 that the T_1/T_2 ratio for the α carbons and other nonmobile carbons of a protein rises sharply as the magnetic field strength increases. Thus, even though there is greater
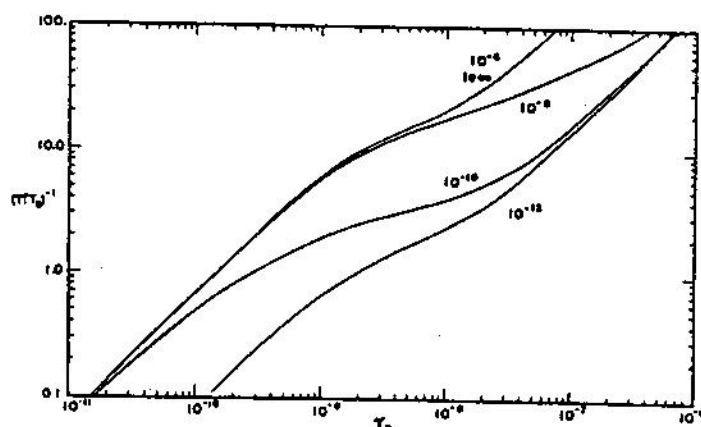

FIGURE 4. Log-log plot of the natural line width (in Hz) vs. τ_R (in sec), for different values of τ_G. (See legend of FIGURE 2 and Reference 11 for details.)

basic sensitivity at high field strengths, the signal-to-noise ratio may be lower, if $\tau_{eff} \gtrsim 10^{-8}$ sec. The T_1 values of FIGURE 5 are those of a methine carbon. To get the corresponding values for methylene and methyl carbons, divide the T_1 values of FIGURE 5 by two and three respectively. On the other hand, nonprotonated carbons will have much longer T_1 values than those shown in FIGURE 5 because the dipolar contribution to $1/T_1$ is inversely proportional to the sixth power of the carbon-hydrogen distance.

The theoretical results of FIGURE 5 do not apply if there are internal rotations with rates comparable to or greater than that of overall molecular reorientation. In FIGURE 6 we show [13]C T_1 values at 14.1 kG for a tetrahedral methine carbon with one degree of internal motion, as a function of the
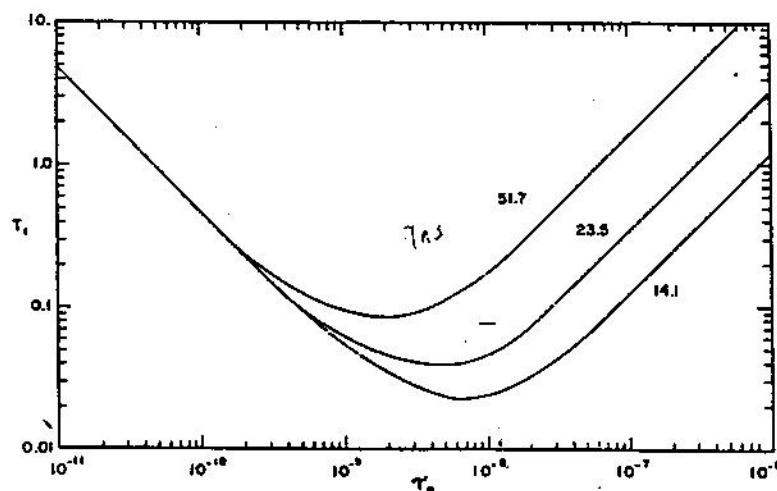

FIGURE 5. Log-log plot of T_1 vs. τ_R (both in sec). (See legend of FIGURE 1 and Reference 11 for details.)

correlation time for overall rotation (τ_R) for different values of the correlation time for internal rotation (τ_G). In FIGURE 7 the T_1 values are plotted against τ_G, for different values of τ_R. Fast internal rotation ($\tau_G \ll \tau_R$) produces a longer T_1 than one would have in the absence of internal motions. However, for $\tau_R \gtrsim 5 \times 10^{-8}$ sec, T_1 first gets shorter at the onset of internal rotation, and then T_1 goes through a minimum as the rate of internal rotation increases (FIGURE 7). One should also note that FIGURES 6 and 7 are valid only when there is one degree of internal motion, and only for a tetrahedral angle between the C-H vector and the axis of internal rotation. Results for other angles can be readily calculated,[11] but the calculations get more tedious for more than one degree of internal motion.[20]
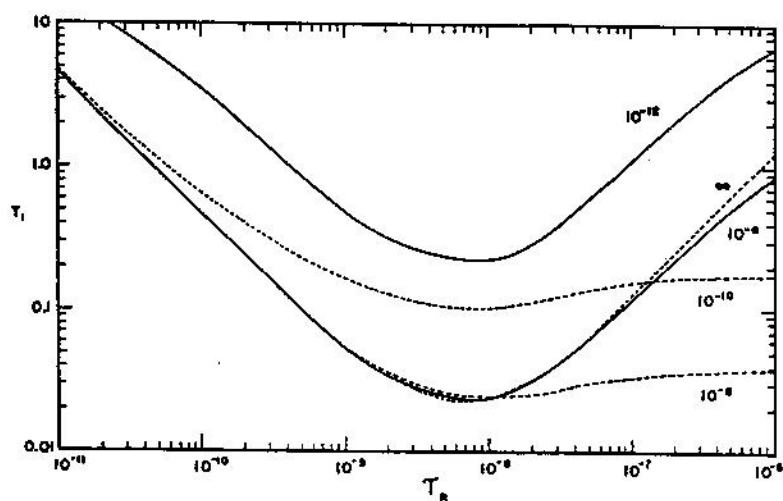
FIGURE 6. Log-log plot of T_1 vs. τ_R for different values of τ_G. (See legend of FIGURE 2 and Reference 11 for details.)
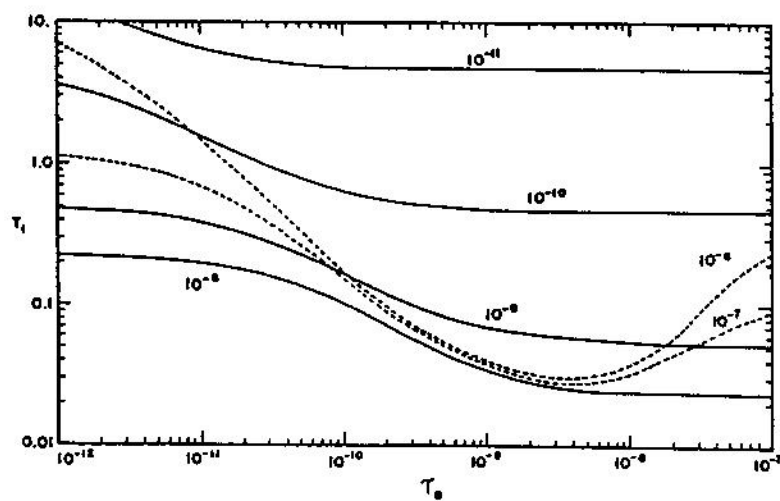

FIGURE 7. Log-log plot of T_1 vs. τ_G for different values of τ_R. (See legend of FIGURE 2 and Reference 11 for details.)

Observation of Single-Carbon Resonances of Proteins

The results of the previous sections indicate that the best opportunities for observing single-carbon resonances of proteins are presented by nonprotonated carbons and by protonated carbons with several degrees of internal freedom. All carbons in the latter category are saturated side-chain carbons which fall in a region of the ^{13}C spectrum crowded with hundreds of protein resonances. Moreover, chemical shift nonequivalence from protein folding, a necessary condition for resolving single-carbon resonances, is least likely to occur for carbons with appreciable internal mobility. We do not discount the possibility of studying single-carbon resonances of saturated side chains, especially methyl groups. We have concentrated our present efforts in the region of nonprotonated carbons. The only nonprotonated carbons of amino acid residues are the following: (1) the amide carbonyl carbons of the protein backbone; (2) the C-terminal carboxyl carbon; (3) the amide carbonyl side-chain carbons of Asn and Gln; (4) the carboxyl side-chain carbons of Asp and Glu; (5) the ζ-carbon of Arg; (6) the γ-carbons of His and Phe; (7) the γ and ζ-carbons of Tyr; (8) the γ, δ_2, and ϵ_2-carbons of Trp. The first four categories normally produce ^{13}C resonances in the range 10–25 ppm upfield from CS_2.[5, 12] We have not yet attempted to identify single-carbon resonances in this region. The ζ-carbons of arginine residues resonate at about 36 ppm upfield from CS_2. The aromatic carbons (categories 6–8) normally resonate in the range 37–85 ppm upfield from CS_2.[5, 12, 22, 23]

It appears to us that nonprotonated aromatic carbons hold the most promise for observing resolved single-carbon resonances because they cover a relatively large range of chemical shifts for a small number of carbons. The resonances of protonated aromatic carbons are in close proximity to many nonprotonated ones. On the basis of arguments presented in the section on line widths, however, we expect the protonated carbons to yield broad resonances which do not seriously interfere with the detection of the narrow nonprotonated carbons.

Unfortunately, on the basis of arguments presented earlier, we expect little if any nuclear Overhauser enhancement for aromatic carbons of native proteins. In this case, as explained the section on nuclear Overhauser enhancement, commercial Fourier transform nmr equipment is inadequate for studying single-carbon resonances of proteins. We decided that the most practical approach to this problem was the development of a probe for very large spinning sample tubes. A sample tube with an outside diameter of 20 mm was chosen.[24] The probe was incorporated into our existing "home-built" Fourier transform nmr spectrometer,[1, 15, 24] operating at 14.2 kG (15.18 MHz ^{13}C resonance frequency). With the 20 mm probe, we can achieve a given signal-to-noise ratio in about one-ninth the time required on commercial Fourier transform nmr instruments operating at 21–24 kG. The magnetic field homogeneity over our large sample volume (about 10–12 ml) is remarkably good.[24] About 0.3 Hz inhomogeneity broadening can be achieved routinely in our Varian 12-inch electromagnet, of the type used in HR-60, HA-60, DP-60, and DA-60 spectrometers. We use no homogeneity correction coils other than those supplied by the manufacturer. We can now detect single-carbon resonances of small proteins in less than six hours of signal accumulation time. The price we pay for this sensitivity is the very large amount of sample required for our 20 mm probe.

FIGURE 8 shows a proton-decoupled natural-abundance ^{13}C spectrum of 15 mM aqueous hen egg-white lysozyme ($C_{613}H_{950}N_{192}O_{184}S_{10}$, 14,306 MW) obtained with 2 Hz digital resolution, after 5.8 hr of signal accumulation. Overall assignments of the various spectral regions can be made on the basis of published data.[1-7, 12, 22] The carbonyl resonances are 10–25 ppm upfield from CS_2. The C^ζ resonance of the eleven arginine residues occurs at about 36 ppm. The saturated carbons resonate above 100 ppm upfield from CS_2. Here we will be concerned only with the aromatic carbon resonances in the range 37–85 ppm. On the basis of known ^{13}C chemical shifts[1, 5, 7, 12, 22, 23] C^ζ of the three tyrosine residues can be assigned to a two-carbon resonance at 37.6 ppm and a single-carbon resonance at 39.6 ppm (FIGURES 8 and 9A). The C^γ resonances of the six tryptophan residues are easily assigned to four single-carbon resonances and one two-carbon resonance in the range 81–85 ppm upfield from CS_2 (FIGURES 8 and 9A). Details are given further on.
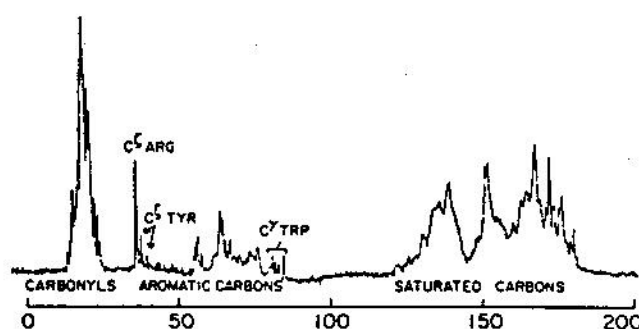

FIGURE 8. Proton-decoupled natural-abundance ^{13}C Fourier transform nmr spectrum of native hen egg-white lysozyme (about 15 mM, 22% w/v in 0.1 M aqueous NaCl, pH 4.0, 42° C) at 15.18 MHz, in a 20 mm sample tube, recorded with 2 Hz digital resolution, after 32,768 accumulations with a recycle time of 0.64 sec (5.8 hr total time). Horizontal scale is in ppm upfield from CS_2.

There are 87 aromatic carbons in hen egg-white lysozyme, arising from one histidine, three phenylalanine, three tyrosine, and six tryptophan residues. Only 28 out of these 87 carbons are nonprotonated. FIGURE 9A shows the region of unsaturated carbons of lysozyme, recorded with 1 Hz digital resolution (twice the resolution of FIGURE 8), after 9.9 hr signal accumulation. The aromatic region of the spectrum contains a number of sharp resonances (peaks 1–22 in FIGURE 9A). It also contains a background of broad peaks approximately in the range 60–80 ppm upfield from CS_2. The theoretical considerations of the section on line widths can be used to conclude that the 28 nonprotonated aromatic carbons give rise to peaks 1–22, and that the 59 protonated carbons produce the broad background. We have verified this expectation experimentally[22] by means of noise-modulated off-resonance proton decoupling,[23] which selectively broadens protonated carbons.

Partial assignment of peaks 1–22 can be made by comparisons with ^{13}C chemical shifts of amino acids[1, 5, 12] and small peptides.[5, 23] Our results show
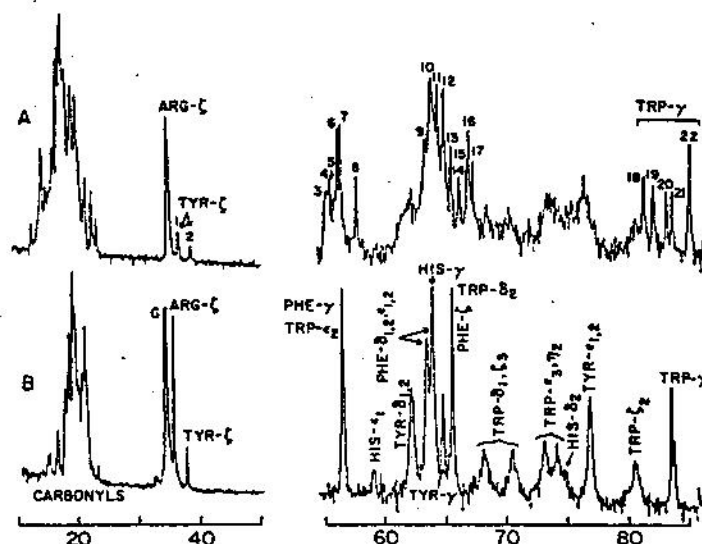
FIGURE 9. Unsaturated-carbon region in the proton-decoupled natural-abundance
[13]C Fourier transform nmr spectra of hen egg-white lysozyme (about 15 mM) at
15.18 MHz in a 20 mm sample tube, recorded with 1 Hz digital resolution, after
32,768 accumulations with a recycle time of 1.09 sec (9.9 hr total time). A: Native
lysozyme, in 0.1 M NaCl, pH 4.0, 42° C. Narrow aromatic carbon resonances, iden-
tified by noise-modulated off-resonance proton-decoupling (spectrum not shown), are
numbered consecutively from left to right. B: Guanidine denatured lysozyme, in 0.1
M NaCl and 6.5 M guanidinium chloride, pH 3.9, 54° C. Horizontal scale is in ppm
upfield from CS_2. Assignments of nonprotonated aromatic carbons are given with
horizontal lettering. Assignments of aromatic methine carbons are shown vertically.
Standard IUPAC-IUB designations for amino acid carbons are used. Peak G is the
resonance of the guanidinium ion.

that folding of a protein into its native conformation can produce large [13]C
chemical shift nonequivalence. The two C^ζ resonances of the three tyrosine
residues, peaks 1 and 2 of FIGURE 9A, are shifted 0.6 ppm downfield and
1.4 ppm upfield, respectively, from their common position at 38.1 ppm upfield
from CS_2 in the spectrum of denatured lysozyme (FIGURE 9B). Peaks 18–22
in the spectrum of native lysozyme (FIGURE 9A) can be assigned to C^γ of
the six tryptophan residues. Clearly, peaks 18–21 are single-carbon resonances,
and peak 22 is a two-carbon resonance. The changes in chemical shift with
respect to their nearly coincident position at about 83.8 ppm in the spectrum
of denatured lysozyme (FIGURE 9B) are: 2.4 ppm downfield (peak 18),
1.7 ppm downfield (peak 19), 0.6 ppm downfield (peak 20), no measurable
change (peak 21), and 1.4 ppm upfield (peak 22). These values are subject
to an error of up to ±0.2 ppm, because of slight splitting of the C^γ resonance
in the spectrum of denatured lysozyme. Peaks 18 and 19 of native lysozyme
(FIGURE 9A) overlap with a broad resonance assignable to $C^{\Gamma 2}$ of the trypto-
phan residues. Peaks 3–8 contain the resonances of C^γ of the phenylalanines
and $C^{\epsilon 2}$ of the tryptophans, a total of 9 carbons. Peaks 9–17 contain the
resonances of C^γ of the histidine and the tyrosines and $C^{\delta 2}$ of the tryptophans,

a total of 10 carbons for 9 peaks. They overlap with a large number of broad protonated-carbon resonances. It is likely that the region of peaks 10–12 contains four nonprotonated carbons, while peaks 9 and 13–17 are all single-carbon resonances.

We have calculated the effect of aromatic ring currents [26] on the ^{13}C chemical shifts of native lysozyme, with the assumption that the conformations in the crystal and in solution are the same. Our procedure is analogous to that used by Sternlicht and Wilson [27] for calculations of the proton nmr spectral envelopes. Most of our calculated ring-current effects are approximately an order of magnitude smaller than the observed ^{13}C chemical shift nonequivalences produced by folding into the native conformation. The discrepancy indicates either that ring-current effects are not major contributing factors to the observed ^{13}C chemical shift nonequivalence in native lysozyme or that the approximations used in our calculations [26, 27] are not valid. This question merits further study.

We have also studied the proton-decoupled natural-abundance ^{13}C spectra of horse-heart cytochrome *c* in the diamagnetic and paramagnetic forms. The region of unsaturated carbon resonances (excluding carbonyls) of ferrocytochrome *c* is shown in FIGURE 10. The spectrum was obtained in 11.4 hr of signal accumulation time, using a 20% w/v aqueous solution. The C$^\gamma$ resonance of the single tryptophan (residue 59) is clearly observable. Spectra recorded with noise-modulated off-resonance proton-decoupling [25] indicate that all the narrow resonances arise from nonprotonated carbons. The number of narrow resonances is significantly greater than the 20 unsaturated carbons of the two arginine, four tyrosine, four phenylalanine, one tryptophan, and three histidine residues. The additional resonances must originate from nonprotonated carbons of the porphyrin. The spectrum of ferricytochrome *c* contains
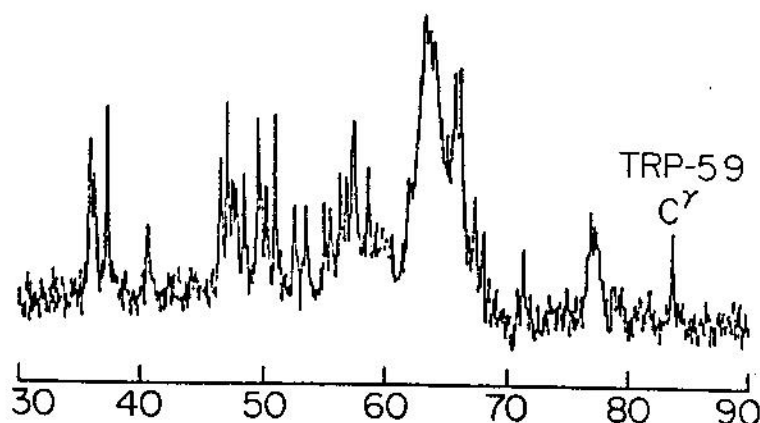

FIGURE 10. Region of aromatic carbons (and C$^\zeta$ of Arg) in the proton-decoupled natural-abundance [13]C Fourier transform nmr spectrum of reduced horse-heart cytochrome *c* (about 20% w/v solution in phosphate buffer, pH 6.6, 37° C) at 15.18 MHz, in a 20 mm sample tube, recorded with 1.8 Hz resolution, after 35,533 accumulations with a recycle time of 1.16 sec (11.4 hr total time). Horizontal scale is in ppm upfield from CS$_2$.

fewer sharp peaks, presumably because the porphyrin carbon resonances are broadened beyond detection. Further studies of cytochrome c are in progress.

CONCLUSION

We have shown that with the use of our 20 mm probe it is practical to attain sufficient signal-to-noise ratios for detection of single-carbon resonances in proton-decoupled natural-abundance ^{13}C Fourier transform nmr spectra of proteins. We have also shown that nonprotonated aromatic carbons of a native protein yield narrow ^{13}C resonances, whereas protonated aromatic carbons yield broad resonances, a feature that simplifies the interpretation of the aromatic region of the spectrum. Finally, we have demonstrated that the folding of a protein into its native conformation may produce sufficient chemical shift nonequivalence to make possible the observation of numerous resolved single-carbon resonances in the aromatic region of the ^{13}C spectrum. The way is now open for probing protein properties in solution by means of ^{13}C chemical shifts, line widths, and spin-lattice relaxation times of individual carbon sites.

REFERENCES

1. ALLERHAND, A., D. W. COCHRAN & D. DODDRELL. 1970. Proc. Natl. Acad. Sci. USA 67: 1093–1096.
2. ALLERHAND, A., D. DODDRELL, V. GLUSHKO, D. W. COCHRAN, E. WENKERT, P. J. LAWSON & F. R. N. GURD. 1971. J. Amer. Chem. Soc. 93: 544–546.
3. CHIEN, J. C. W. & J. F. BRANDTS. 1971. Nature New Biol. 230: 209–210.
4. CONTI, F. & M. PACI. 1971. FEBS Letters 17: 149–152.
5. GLUSHKO, V., P. J. LAWSON & F. R. N. GURD. 1972. J. Biol. Chem. 247: 3176–3185.
6. MOON, R. B. & J. H. RICHARDS. 1972. Proc. Natl. Acad. Sci. USA 69: 2193–2197.
7. FREEDMAN, M. H., J. R. LYERLA, I. M. CHAIKEN & J. S. COHEN. 1973. Eur. J. Biochem. 32: 215–226.
8. ROBERTS, G. C. K. & O. JARDETZKY. 1970. Advan. Protein Chem. 24: 447–545.
9. STOTHERS, J. B. 1972. Carbon-13 nmr Spectroscopy. Academic Press. New York. N.Y.
10. KUHLMANN, K. F., D. M. GRANT & R. K. HARRIS. 1970. J. Chem. Phys. 52: 3439–3448.
11. DODDRELL, D., V. GLUSHKO & A. ALLERHAND. 1972. J. Chem. Phys. 56: 3683–3689.
12. HORSLEY, W., H. STERNLICHT & J. S. COHEN. 1970. J. Amer. Chem. Soc. 92: 680–686.
13. ERNST, R. R. & W. A. ANDERSON. 1966. Rev. Sci. Instr. 37: 93–102.
14. LEVY, G. C. & G. L. NELSON. 1972. Carbon-13 Nuclear Magnetic Resonance for Organic Chemists. Wiley-Interscience. New York. N.Y.
15. ALLERHAND, A., D. DODDRELL & R. KOMOROSKI. 1971. J. Chem. Phys. 55: 189–198.
16. LYERLA, J. R. & D. M. GRANT. 1972. Carbon-13 nuclear relaxation. In Magnetic Resonance. C. A. McDowell. Ed. MPT Review of Physical Chemistry (Series One). 4: 155–200. University Park Press. Baltimore, Md.
17. SOLOMON, I. 1955. Phys. Rev. 99: 559–565.
18. BROWNE, D. T., G. L. KENYON, E. L. PACKER, D. M. WILSON & H. STERNLICHT. 1973. Biochem. Biophys. Res. Commun. 50: 42–47.

19. ALLERHAND, A. & E. OLDFIELD. Biochemistry 12: 3428–3433.
20. WALLACH, D. 1967. J. Chem. Phys. 47: 5258–5268.
21. DODDRELL, D. & A. ALLERHAND. 1971. J. Amer. Chem. Soc. 93: 1558–1559.
22. ALLERHAND, A., R. F. CHILDERS & E. OLDFIELD. 1973. Biochemistry 12: 1335–1341.
23. GLUSHKO, V. G., F. R. N. GURD, P. KEIM, P. J. LAWSON, R. C. MARSHALL, A. M. NIGEN & R. A. VIGNA. 1973. Private communication.
24. ALLERHAND, A., R. F. CHILDERS, R. GOODMAN, E. OLDFIELD & X. YSERN. 1972. Amer. Laboratory 4(11): 19–26.
25. WENKERT, E., A. O. CLOUSE, D. W. COCHRAN & D. DODDRELL. 1969. J. Amer. Chem. Soc. 91: 6879–6880.
26. JOHNSON, C. E. & F. A. BOVEY. 1958. J. Chem. Phys. 29: 1012–1014.
27. STERNLICHT, H. & D. WILSON. 1967. Biochemistry 6: 2881–2892.

DISCUSSION

DR. WILSON (*University of California, Berkeley. Calif.*): Along the lines of complementary techniques in signal enhancement, I would like to mention dual phase detection, in which you have two phase detectors working in quadrature in the final stage of audio detection. We've incorporated this into our XL 100 apparatus and there are some features that I would like to mention. First, it is equivalent to having a pulse amplifier about four times more powerful, because you can pulse in the middle of a spectrum and not lose the detectable magnetization as a function of frequency.

DR. ALLERHAND: Our 90 degree pulse is 15 microseconds, which is adequate to cover a range four or five times that of ^{13}C chemical shifts at 15 MHz.

DR. WILSON: Furthermore, you don't lose resolution by needing twice the memory because by pulsing in the middle you can sample at half the rate in each channel. The third feature, as Professor Redfield mentions in his article on magnetic resonance, is that you can take two real transforms instead of a complex transform, which means that the software doesn't have to have any substantial modifications. Lastly, it's quite inexpensive; the most costly item was a dual rather than a single four-pole filter.

DR. ALLERHAND: In practice have you achieved the 40% improvement in sensitivity that this should have?

DR. WILSON: In practice we have achieved more than that. We thought we would achieve an increase of just a square root of 2, but in practice we achieved between a square root of 2 and 2 because of the magnetization improvement as a function of not being as far from the pulse.